nature portfolio

Peer Review File

Using bacterial population dynamics to count phages and their lysogens

Reviewer #1 (Remarks to the Author):

I commend the authors for this well-written, easy to understand manuscript that provides an alternative to the tedious phage plaque assays and one step growth curves. The approach they suggest is simple, clever, and rigorously supported with data. Given that many phage labs are increasingly using plate readers in their work, this approach should be broadly utilizable. My only suggestion is to remove the sentence at line 150-151. I am fairly certain I have seen published quantitative tests of the connection between slow growth and lysogeny, and besides, the claim adds nothing to the manuscript.

Reviewer #2 (Remarks to the Author):

The paper by Geng et al. tried to propose new assays to quantify phage concentrations and other basic parameters that characterise phage-bacteria interaction by measuring OD and analysing it using mathematical models without involving labor-intensive classical assays. If such a method is established, it will have a significant impact on quantitative phage research. However, I have significant concerns about the proposed method.

My biggest overall concern is that the data is not constraining the model enough; it is overfitting. The authors give the best-fitted value based on simulated annealing with a very small error bar, but it is very likely that there are a wide set of parameters that can do roughly as good, and we cannot use this as a method to infer the parameter.

My other fundamental concern is how the growth rate dependence of parameters is inferred. The experiments are done under the condition that the growth rate is continuously changing, and the authors plot a correlation between the instantaneous growth rate at a specific time point and the inferred parameter. This is only a correlation, and that does not mean that the instantaneous growth rate determines the phage parameter. However, the manuscript does not distinguish between correlation and causality.

I do believe in the usefulness of simple mathematical models, but it is also important to know the limit. In this work, it appears that the model and fits are used beyond their limit.

Below I detail my criticisms.

1)The main finding is that lysis OD is proportional to the logarithm of the initial phage concentration, and by measuring lysis OD by using a plate reader, one can infer the phage concentration without performing the classical plaque experiments. This is a very nice finding and an efficient method of knowing the order of magnitude of the phage concentration. However, the precision is rather limited since the correspondence is only a logarithm. A small error in OD measurement will give a very large error in the readout of the phage concentration. However, the authors do not discuss the precision of the proposed method, which is a very important point if this method were to be used to quantify phage concentration. What is the expected error bar if one measures the lysis OD only once and reads the phage concentration out? Does it help to do many parallel OD curves and measure lysis OD with a smaller error bar?

What percentage of difference in phage concentration can the method detect?

2)The model is based in the cell number concentration, and the authors seems to assume the conversion factor that OD 1 is 10^9 CFU/ml (Supll. Material 6.1) without experimentally checking it. However, it is well known that cell size changes upon growth, especially close to the entropy to the stationary phase, and also depending on the growth media (faster growth gives bigger cells hence, the same OD means less number of cells per mL). This can affect the fitting and, hence, the inferred parameters for some factors.

3)In figure 2, the authors tried to infer the latent period, burst size, and the rate constant for phage/cell encounter by fitting the model to OD and phage concentration curve.

3-a)There is a fundamental question if the infected cells in the latent period contribute to the OD in the same way as uninfected cells. The last author previously showed impressive movies of cells infected by lambda going through the lysis process (Golding I. Single-cell studies of phage λ: hidden treasures under Occam's rug. Annual Review of Virology. 2016 Sep 29;3:453-72.), and those examples cells are clearly significantly longer than typical uninfected E. coli before the burst. The current model assumes that one infected cell represents the same OD as one infected cell, but this can be wrong if the cell size is significantly different, and that can affect the inference of the parameter.

3-b)To infer the latent period, a model was fitted to the OD curve of phage-infected cultures from its deviation from the uninfected OD curve to the collapse using the model presented in 6.3 in the supplementary material. It is unclear how the initial condition for eq. (6.5) was set. If it was set so that all populations are in I1 at the lysis OD, then that is equivalent to assuming that all the cells were infected at the start of the fitting simultaneously (the peak of the OD curve). If so, even if my concern a) were not significant, the fit underestimates the latent period; fit starts when the visible lysis starts to occur, so that means a significant number of cells were infected at lysis peak timing minus the latent period. A few more concerns regarding this fit are:

3-b-i)The authors make a correlation curve between the instantaneous growth rate at the lysis OD and the inferred latent period, but as stated above, the actual infection should have happened over a period of time where the growth rate is continuously changing. Because the nutrient decreases over time in general, the latent period can still correlate with the growth rate at the lysis OD, but that does not mean that the instantaneous growth rate at that time determines the latent period. However, the authors assume this causality without deeper consideration.

3-b-ii)The authors state that the fitted value of tau increases with the doubling time at the massive lysis and state it is T4 measurement in ref. 22. However, another measurement of T4 parameters in various steady-state growth reported different tendencies (Hadas H, Einav M, Fishov I, Zaritsky A. Bacteriophage T4 development depends on the physiology of its host Escherichia coli. Microbiology. 1997 Jan;143(1):179-85. : Parameter dependence is summarised in Rabinovitch A, Fishov I, Hadas H, Einav M, Zaritsky A. Bacteriophage T4 development in Escherichia coli is growth rate dependent. Journal of theoretical biology. 2002 May 7;216(1):1-4.). This should be discussed.

4) The model presented in Fig.2 is used to fit the phage concentration curve in Fig. 2D.

4-a)The model assumes that the phages are produced only after the cell lysis. However, the method states that to measure the phage concentration in Fig. 2D, the cells in the sample were lysed by adding chloroform. This allows the phages produced in the infected cells that have not yet burst also to be included in the phage count. Therefore, the data in Fig. 2D is not correspond to the free phage P in the model used in the fitting.

4-b)I assume that the authors used the latent period for this fit based on the instantaneous growth rate and the correlation in Fig. 2C. This has the concern as stated in 2-ii); hence, the value used may be wrong.

4-c) The authors can still fit the curve despite the above uncertainties and state the best-fit parameters with very small error bars. This can be a sign of overfitting; because of a high degree of freedom and many parameters can compensate for each other, there may be a wide range of parameters that fit quite all right, but authors are only picking the best fit. In reality, the parameters are not as constrained as the error bars suggest. For example, the authors assume constant burst size, but a clear change in the burst size was observed when the growth rate was changed in the steady state growth condition in the Hadas paper mentioned above. For example, if the latent period prediction in Fig 2C is wrong but actually does not change much, but if burst size is reduced with growth rate, this may compensate. Overall, there are so many uncertainties in the model and the fit, and inferring parameters with the error bar that the authors present appears misleading.

5) In Fig 4, the authors inferred the growth rate dependence of the lysogenisation frequency and the spontaneous induction rate.

5-a)For Fig. A-C, the authors plot a correlation between the frequency of lysogeny and the growth rate at the time when the phage is added. Again, as stated above, this is just a correlation.
The model presented in Fig. S9 is inconsistent with their assumption of the lysogenisation frequency dependence upon growth rate and MOI.
5-b)The model does not count the superinfection (though it is possible to construct such a model, where every infection to the infected state can move to another superinfected state), so the model does not know how many fraction of the infected cells experienced superinfections. Instead, the lysogenisation frequency is assigned based on the initially added phage concentration. This is another indication that the data is not constraining the model: A simple model actually reproduces the curves quite all right without the complex growth rate dependence or MOI dependence. That does not necessarily mean that the model and inferred parameters are close to the truth.

5-c)For the induction rate, the authors assume there is no phage adsorption in this experiment. The method states that LB medium was “supplemented with 10mM $MgSO_4$ and 0.2% glucose, the latter added to inhibit phage adsorption to cells (ref 13, 35)”. In ref. 35, the effect on the adsorption rate to add glucose is at most factor 100 reduction, but it can be only factor 10. When the cell concentration is high and investigating time scale of hours, even a small adsorption rate can affect the phage number significantly. The authors should show that the adsorption is negligible in the concentration and time scale used in the condition used.

Reviewer #1

"I commend the authors for this well-written, easy to understand manuscript that provides an alternative to the tedious phage plaque assays and one step growth curves. The approach they suggest is simple, clever, and rigorously supported with data. Given that many phage labs are increasingly using plate readers in their work, this approach should be broadly utilizable.

"**[1.0]** My only suggestion is to remove the sentence at line 150-151. I am fairly certain I have seen published quantitative tests of the connection between slow growth and lysogeny, and besides, the claim adds nothing to the manuscript."

We have rewritten the sentence in question (line 229). More broadly, our discussion of the relation between growth rate and lysogeny has been revised following input from the second reviewer (see **comments 2.0-b** and **2.5-a** below). The new text is found in lines 225-229 of the manuscript.

Reviewer #2

"The paper by Geng et al. tried to propose new assays to quantify phage concentrations and other basic parameters that characterise phage-bacteria interaction by measuring OD and analysing it using mathematical models without involving labor-intensive classical assays. If such a method is established, it will have a significant impact on quantitative phage research. However, I have significant concerns about the proposed method.

[2.0-a] My biggest overall concern is that the data is not constraining the model enough; it is overfitting. The authors give the best-fitted value based on simulated annealing with a very small error bar, but it is very likely that there are a wide set of parameters that can do roughly as good, and we cannot use this as a method to infer the parameter."

In response to the reviewer's comments, we have significantly revamped our procedure for model fitting and parameter inference. As detailed below, we now consider explicitly the uncertainty in model structure and parameters. Crucially, we find that this uncertainty does not hamper the interpretability of the model or its predictive power. In particular:

1. Uncertainty in model structure. Previously, when modeling infection in rich media, we imposed a dependence of the latent period τ on the cell growth rate. However, as pointed out by the reviewer (**comment 2.4-c** below), the dependence on growth rate may appear through the other infection parameters, namely, the phage-cell encounter rate r or burst size B. To explore this uncertainty in model structure, we now test a null model, where all parameters are independent of the normalized instantaneous growth rate φ, and three models ("r-model", "B-model", and "τ-model") in which one of the infection parameters (r, B, τ) is assumed to be a linear function of φ, with the slope and intercept of that linear function as free parameters; see lines 89-101 of the revised text and **Supplementary Methods, Sections 6.3-6.5**.

Fitting each of these models to the OD dynamics of infected cultures, and examining the mean squared error (MSE), we found that the null model fails to capture the data (**NEW Supplementary Fig. 7a**, reproduced below), whereas the models where either r, B or τ vary linearly with growth rate all capture the data well, with comparable MSE (**Fig. 3c**, **NEW Supplementary Figs. 7b-c**, and **NEW Fig. 3d**, all reproduced below).

Model fitting thus indicates that infection parameters depend on the instantaneous growth rate. While the procedure does not reveal through which of these parameters the dependence arises, analyzing parameter uncertainty (Point 2 below) indicates that, in the regime of fast cell growth (doubling time $\lesssim$ 30 min), the three model variants yield a comparable range of values for r, B, and τ (**NEW Supplementary Fig. 8**, reproduced under Point 2 below). Furthermore, as we describe below (Point 3), each of the three models is able to successfully predict—rather than merely fit—the experimental phage dynamics (**NEW Fig. 3d** and **NEW Supplementary Figs. 7e-f**, all reproduced below). Thus, the uncertainty in the model structure and parameters does not diminish its predictive power (a property which mirrors the performance of other so-called "sloppy models" in systems biology[1]). Finally (Point 4), the three model variants capture the same underlying behavior of a single coarse-grained parameter, the relative growth rate of the viral population, $R = \frac{r \cdot B}{\exp(\tau \cdot g*)}$, thus offering an intuitive interpretation for the fitting results.

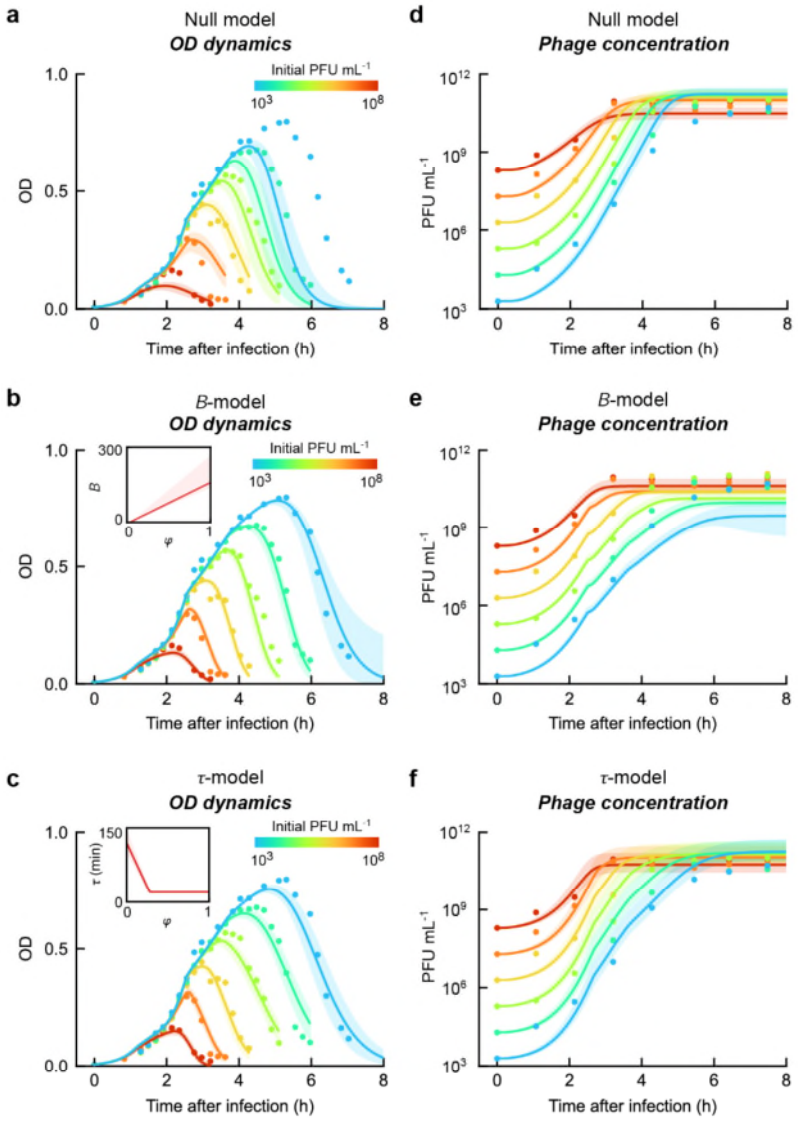

Supplementary Fig. 7: Modeling infection dynamics under different growth-rate dependencies.

(**a-c**) Model fitting for the OD dynamics. The models tested are (**a**) "null model": r, B, and τ are constant, (**b**) "B-model": r and τ are constant, and $B = \max(0,\ B_k \cdot \varphi + B_0)$, and (**c**) "$\tau$-model": r and B are constant, and $\tau = \max(20,\ \tau_k \cdot \varphi + \tau_0)$. In each panel, colored markers, data from infection at different initial phage concentrations. Colored lines, best fit of the model. Colored shading, fits by the ensemble of parameters obtained using Markov chain Monte Carlo (MCMC). Inset, fitted infection parameter as a function of normalized instantaneous growth rate φ.
(**d-f**) Prediction of the phage dynamics, by the (**d**) "null model", (**e**) "B-model" and (**f**) "τ-model". In each panel, colored markers, data from infection at different initial phage concentrations. Colored lines, model predictions from the best-fit parameters. Colored shading, model predictions from the ensemble of parameters.
The corresponding results for the "r-model" are shown in **Figs. 3c** and **3e**. The fitting and prediction procedures are described in **Supplementary Methods, Sections 6.4-6.6**. The fitted parameters are shown in **Supplementary Table 3**.

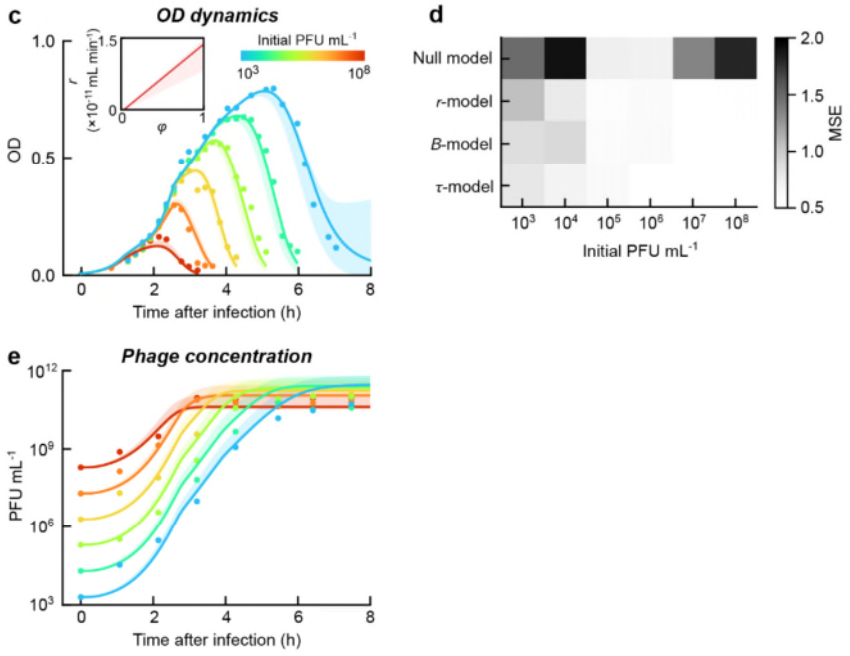

Fig. 3: A mathematical model captures the growth dynamics of phages and bacteria and allows inference of infection parameters.

[...] (**c**) A model where the rate of phage-cell encounter (r) depends on the bacterial growth rate captures the measured OD dynamics in cultures infected by lambda phages. The dependence of r on the normalized instantaneous growth rate of the host cells (ϕ) is described by: $r = \max(0, r_k \cdot \phi + r_0)$. Colored markers, data from infection at different initial phage concentrations. Colored lines, best fit of the model. Colored shading, fits by the ensemble of parameters. Inset, the fitted dependence of r on ϕ. For other model variants, see **Supplementary Fig. 7**.
(**d**) The mean squared error (MSE) of the different model variants when fitting to the measured OD dynamics.
(**e**) The model variant where r depends on the bacterial growth rate successfully predicts the phage concentration over time in the infected cultures. Colored markers, data from infection at different initial phage concentrations. Colored lines, predictions of the best-fit model; shading, predictions by the ensemble parameters. For other model variants, see **Supplementary Fig. 7**.

2. Uncertainty in parameter values. In the original manuscript, the error in parameter values was estimated from repeated runs of the simulated annealing procedure. To explore the parameter space more thoroughly, we now use Markov chain Monte Carlo (MCMC) (ref. [2]) to estimate the posterior distributions of the parameters (see lines 89-90 of the revised text and **Supplementary Methods, Sections 6.4-6.5**). The results for infection in LB supplemented with 10 mM $MgSO_4$ (LBM), shown in **NEW Supplementary Fig. 8** and **Supplementary Table 3** (both reproduced below), indicate a ~3–5 fold uncertainty range for r, B, and τ. Furthermore, as noted in Point 4 below, the coarse-grained parameter $R = \frac{r \cdot B}{\exp(\tau \cdot g*)}$, describing the relative growth rate of the viral population (**Supplementary Methods, Sections 6.7**), is constrained more tightly. We applied the same fitting procedure for infection in M9 minimal broth supplemented with 0.4% maltose (M9Mal) and with 0.4% glucose (M9Glu) (**Supplementary Figs. 10a-d**, reproduced below, and **Supplementary Table 3**).

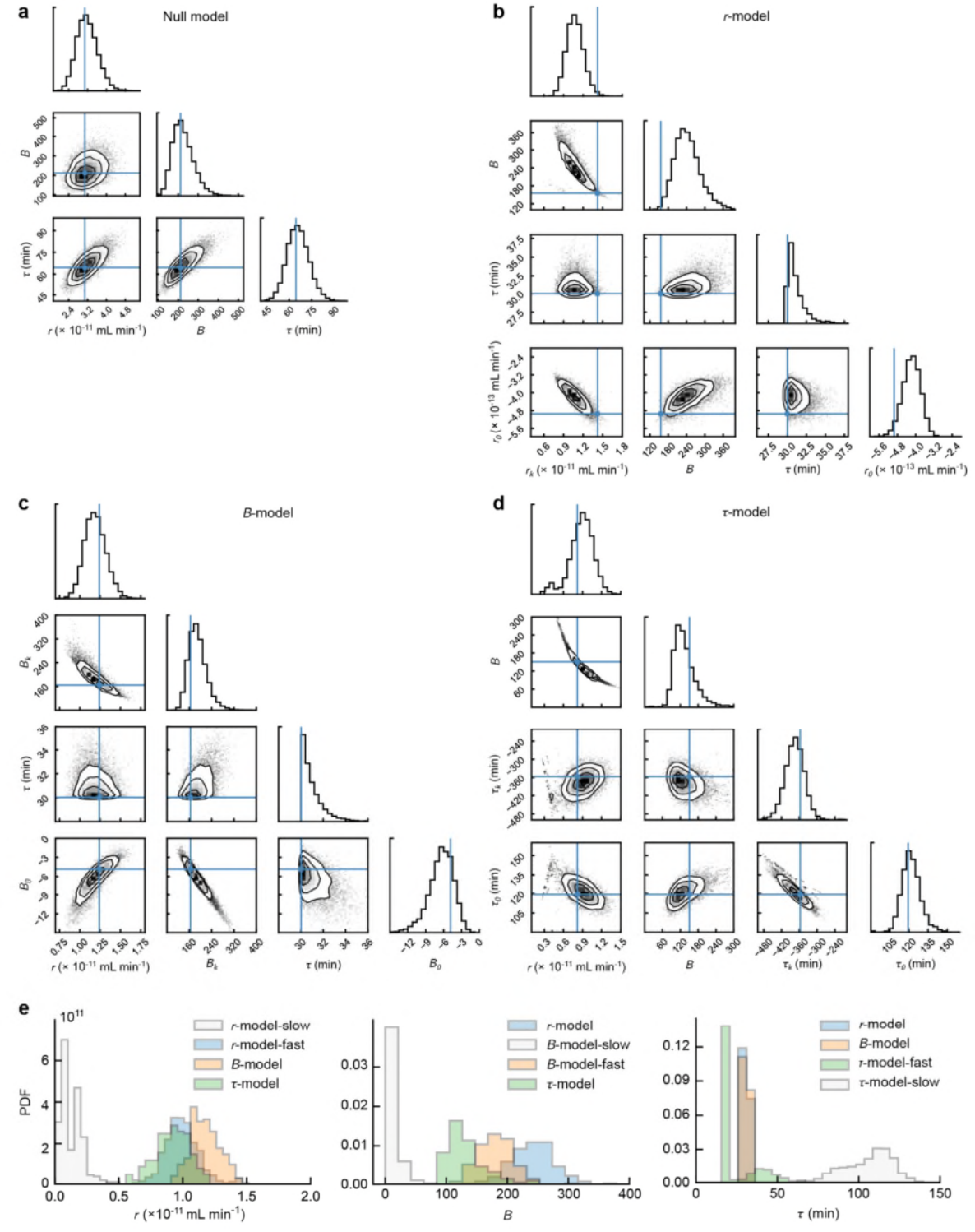

Supplementary Fig. 8: Comparison of inferred parameters under different growth-rate dependencies.

(**a-d**) The distribution of phage-cell encounter rate r, burst size B, latent period τ, and their dependencies on the normalized instantaneous growth rate (φ). The models shown are (**a**) "null model", (**b**) "r-model", (**c**) "B-model" and (**d**) "τ-model". In each panel, the marginal distribution of the parameters is shown on the diagonal, and the joint distribution of pairs of parameters is shown off-diagonal. Blue line indicates the best-fit parameter value.
(e) Comparison of the distribution of r (left), B (middle), and τ (right) from the different models ("r-model", "B-model" and "τ-model"). For models in which the parameter is growth rate-independent, the posterior distribution from MCMC is shown. For models in which the parameter is growth rate-dependent, we integrate the posterior distribution with the growth rate

distribution throughout the infection processes; the resulting distribution is divided into a population representing the parameters at fast-growing conditions (doubling time $\lesssim$ 30 min) and another population representing the parameters at slow-growing conditions (doubling time $>$ 30 min, in gray).
The fitting procedure is described in **Supplementary Methods, Sections 6.4-6.5**. The fitted parameters are shown in **Supplementary Table 3**.

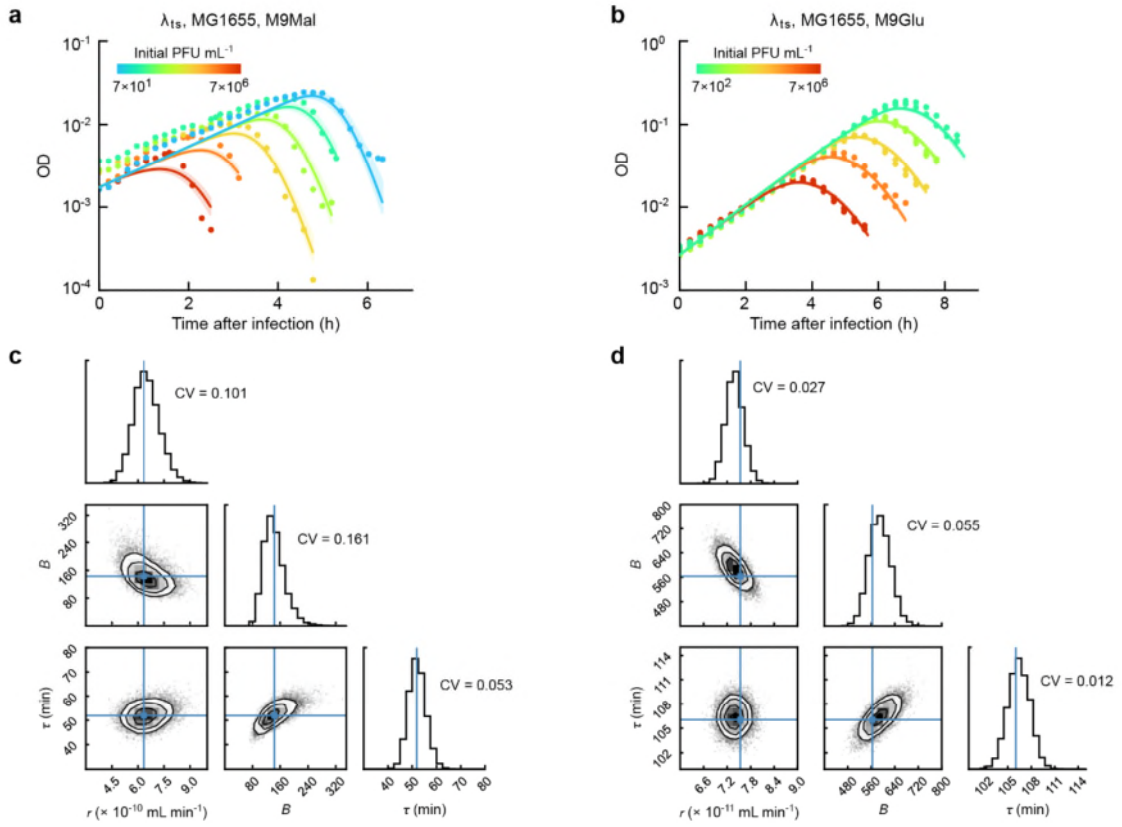

Supplementary Fig. 10: Modeling infection dynamics in minimal media.

(**a-b**) Fitted OD dynamics for infection in (**a**) M9Mal and (**b**) M9Glu. In each panel, colored markers, data from infection at different initial phage concentrations. Colored lines, best fit of the model. Colored shading, fits by the ensemble of parameters obtained using Markov chain Monte Carlo (MCMC).
(**c-d**) The distribution of phage-cell encounter rate r, burst size B, and latent period τ for infection in (**c**) M9Mal and (**d**) M9Glu. In each panel, the marginal distribution of the parameters is shown on the diagonal, and the joint distribution of pairs of parameters is shown off-diagonal. Blue line indicates the best-fit parameter value. The fitting procedure is described in **Supplementary Methods, Section 6.4**. The fitted parameters are shown in **Supplementary Table 3**.

Supplementary Table 3: Fitted infection parameters under different growth conditions

Growth medium	Model	Parameter	Range of prior	Best fit value	Range of ensemble of parameters
LBM	Null model	r	[10^{-12}, 10^{-10}] mL min^{-1}	3.1×10^{-11} mL min^{-1}	[2.4×10^{-11}, 4.1×10^{-11}] mL min^{-1}
		B	[10, 1000]	211.6	[140.5, 344.8]
		τ	[30, 150] min	64.5 min	[52.3, 81.2] min
	r-model: $r = \max(0, r_0 + r_k \cdot \phi)$	r_k	[10^{-12}, 10^{-10}] mL min^{-1}	1.42×10^{-11} mL min^{-1}	[8.5×10^{-12}, 2.4×10^{-11}] mL min^{-1}
		r_0	[10^{-12}, 10^{-10}] mL min^{-1}	-4.9×10^{-13} mL min^{-1}	[$-5e\times10^{-13}$, 2.8×10^{-12}] mL min^{-1}
		B	[10, 1000]	155.7	[96.5, 343.9]
		τ	[30, 150] min	30.0 min	[30.0, 35.3] min
	B-model: $B = \max(0, B_0 + B_k \cdot \phi)$	r	[10^{-12}, 10^{-10}] mL min^{-1}	1.24×10^{-11} mL min^{-1}	[9.4×10^{-12}, 1.5×10^{-11}] mL min^{-1}
		B_k	[10, 1000]	164.2	[143.5, 276.4]
		B_0	[-1000, 1000]	-4.9	[-11.3, -3.2]
		τ	[30, 150] min	30.0 min	[30.0, 34.1] min
	τ-model: $\tau = \max(20, \tau_0 + \tau_k \cdot \phi)$	r	[10^{-12}, 10^{-10}] mL min^{-1}	8.1×10^{-12} mL min^{-1}	[4.3×10^{-12}, 1.2×10^{-11}] mL min^{-1}
		B	[10, 1000]	150.9	[84.6, 370.4]
		τ_k	[-1000, 1000] min	-357.9 min	[-438.7, -298.3] min
		τ_0	[0, 1000] min	119.4 min	[101.8, 142.7] min
M9Mal	Null model	r	[10^{-11}, 10^{-8}] mL min^{-1}	6.3×10^{-10} mL min^{-1}	[5.2×10^{-10}, 7.9×10^{-10}] mL min^{-1}
		B	[10, 1000]	150.0	[97.8, 213.4]
		τ	[30, 150] min	51.8 min	[46.9, 59.1] min
M9Glu	Null model	r	[10^{-11}, 10^{-8}] mL min^{-1}	7.5×10^{-11} mL min^{-1}	[7.0×10^{-11}, 7.8×10^{-11}] mL min^{-1}
		B	[10, 1000]	563.4	[515.9, 661.7]
		τ	[30, 150] min	106.0 min	[103.7, 109.1] min

3. Predictive power of the model. To test the model's predictive power, we now fit it to the OD dynamics, and use the inferred parameters to predict the phage dynamics (lines 102-108 and **Supplementary Methods, Section 6.6**). This contrasts with the earlier version of the manuscript, where we used both cell and phage dynamics in the fit. We find that, regardless of whether r, B, or τ is assumed to depend on the cell's growth rate, model predictions closely capture the phage data (**Fig. 3e**, and **NEW Supplementary Figs. 7d-f**, reproduced in Point 1 above). Thus, the uncertainty in model structure and parameters does not diminish its predictive power (which, as noted above, mirrors the performance of other so-called "sloppy models" in systems biology[1]).

4. Model interpretability. Analyzing infection in minimal media (M9Glu, M9Mal), when we plotted the MCMC-sampled parameters in the space of $(\log_{10} r, \log_{10} B, \tau)$, we noticed that they lie approximately in a single plane, described by $\tau = \alpha * [\log_{10} r + \log_{10} B] + \beta$ (**NEW Supplementary Figs. 10e-f**, reproduced below, lines 111-115 and **Supplementary Methods, Section 6.7**). This indicated that the three parameters were constrained beyond their individual uncertainties. Motivated by this observation, we defined the parameter $R = \frac{r \cdot B}{\exp(\tau \cdot g*)}$, which describes the relative growth rate of the viral population (**Supplementary Methods, Section 6.7**). The parameter g^*, which is inferred from the plane of conserved parameters, is found to be of the same order of magnitude as the maximal bacterial growth rate in the experiment (**Supplementary Methods, Section 6.7**). As expected, R exhibits lower uncertainty (CV) than most of the individual infection parameters (**NEW Supplementary Figs. 10i-j**, reproduced below). While further theoretical investigation is needed to derive the growth rate of phages (in analogy to the approach used for chemostat growth in refs. [3,4]), the analysis above nevertheless suggests that our model fitting provides robust inference of an interpretable infection parameter.

When analyzing infection in LBM, we found that the dependence of R on the normalized instantaneous growth rate, as predicted by the three models where r, B, or τ changes with the growth rate, reflected a similar trend across models (**NEW Fig. 3f**, reproduced below). Furthermore, as we discuss in our response to **comments 2.0-b** and **2.3-b-ii** below, the observed trend agrees with previous reports in T4 (refs. [4,5]). Thus, here too R provides a means of interpreting the model results despite the uncertainty in model structure and parameters. These matters are now discussed in lines 115-124 of the revised text.

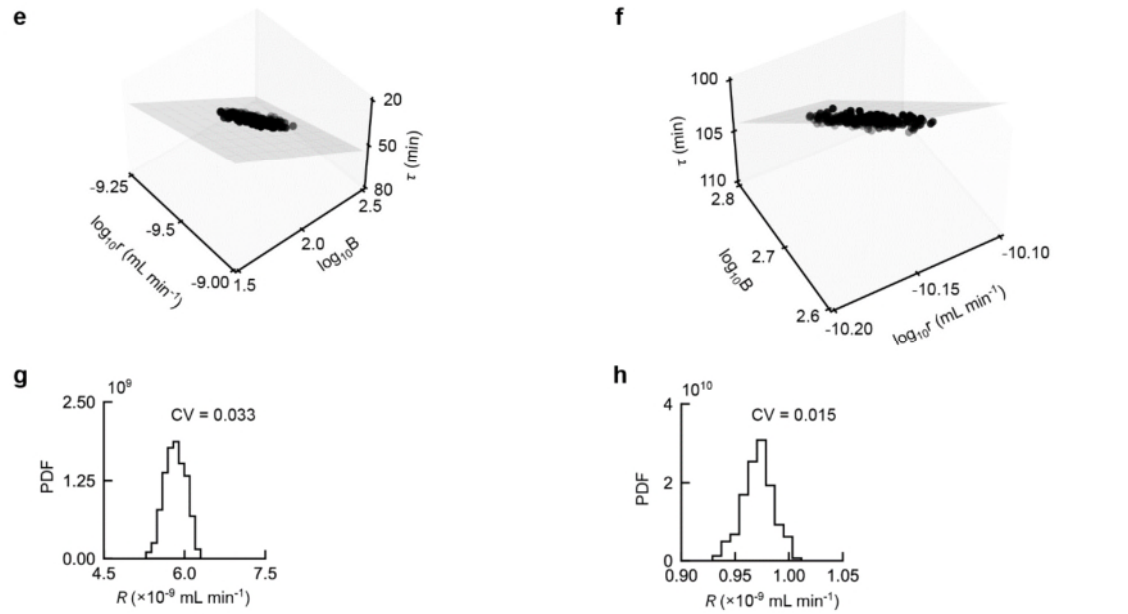

Supplementary Fig. 10: Modeling infection dynamics in minimal media.

[…] (**e-f**) Scatter plot of $\log_{10} r$, $\log_{10} B$ and τ in 3D, for infection in (**e**) M9Mal and (**f**) M9Glu. Markers, the ensemble of parameters obtained using MCMC. Grey shading, fitted plane: $\tau = \alpha * [\log_{10} r + \log_{10} B] + \beta$, where $g^* = \ln 10 / \alpha$. For (**e**) M9Mal, α = 44.1 $\pm$ 0.7, β = -34.1 $\pm$ 1.3, g^* = 0.052 $\pm$ 0.001 min^{-1}. For (**f**) M9Glu, α = 65.0 $\pm$ 1.7, β = 0.02 $\pm$ 2.79, g^* = 0.035 $\pm$ 0.001 min^{-1}.
(**g-h**) The distribution of R for infection in (**g**) M9Mal and (**h**) M9Glu.

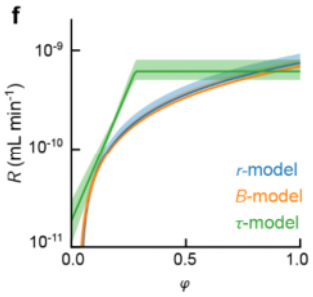

Fig. 3: A mathematical model captures the growth dynamics of phages and bacteria and allows inference of infection parameters.

[...] (**f**) The dependence of the relative growth rate of the viral population (R) on the relative growth rate of the host cells (ϕ). Colored markers, predictions of the best-fit model; shading, predictions by the ensemble of parameters.

"**[2.0-b]** My other fundamental concern is how the growth rate dependence of parameters is inferred. The experiments are done under the condition that the growth rate is continuously changing, and the authors plot a correlation between the instantaneous growth rate at a specific time point and the inferred parameter. This is only a correlation, and that does not mean that the instantaneous growth rate determines the phage parameter. However, the manuscript does not distinguish between correlation and causality."

We cede the point. First, to briefly reiterate from **comment 2.0-a** above, our analysis of infection in rich medium (LBM) indicates that a dependence of infection parameters on growth rate is required for reproducing the experimental data. The inference process leaves unresolved through which specific parameter (r, B, τ) the dependence arises, but the coarse grained parameter $R = \frac{r \cdot B}{\exp(\tau \cdot g^*)}$, capturing the relative growth rate of the viral population (**Supplementary Methods, Section 6.7**), is found to exhibit a similar dependence on growth rate notwithstanding the specific model variant chosen.

The inferred dependence of lambda infection parameters on the cell's growth rate is consistent with experimental reports in other phages[4–6], including the two T4 studies highlighted by the reviewer in **comment 2.3-b-ii** below, both of which modulated the growth rate directly (using chemostat growth in LB in one case[4], batch culture in different carbons sources in the other[5]). When mapped to the same observable—the phage population growth rate, R—the data from both studies indicates an increasing trend of this parameter with growth rate (**NEW Supplementary Fig. 11**, reproduced below), reminiscent of the trend we observed (**NEW Fig. 3f**, reproduced in **comment 2.0-a** above). This similarity in findings makes it plausible that, in our case too, it is the growth rate that modulates infection parameters.

It is nevertheless true that, in our experiments, we cannot delineate the impact of instantaneous growth rate from a possible dependence on the growth history of the culture. Such a dependence can conceivably come about through, e.g., the residual activity of metabolic pathways used by the cells in response to previous nutrient substrates[7], or the accumulation of secreted signaling molecules and metabolites[8–10], which may change the chemical properties of the growth medium over time[11,12]. Our inability to exclude these scenarios is an important caveat, which we now discuss in lines 217-221. Similar considerations also pertain to the relation between growth rate and the propensity to enter and exit lysogeny, discussed in our in response to **comment 2.5-a** below.

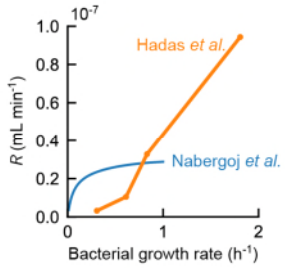

Supplementary Fig. 11: The relative growth rate of phage T4.

The relative growth rate of viral population (R) for phage T4 as a function of bacterial growth rate, calculated from the data reported in Nabergoj *et al.*[4] (blue) and Hadas *et al.*[5] (orange). The data analysis procedure is described in **Supplementary Methods, Section 6.7**.

"I do believe in the usefulness of simple mathematical models, but it is also important to know the limit. In this work, it appears that the model and fits are used beyond their limit.

Below I detail my criticisms.

[2.1] The main finding is that lysis OD is proportional to the logarithm of the initial phage concentration, and by measuring lysis OD by using a plate reader, one can infer the phage concentration without performing the classical plaque experiments. This is a very nice finding and an efficient method of knowing the order of magnitude of the phage concentration. However, the precision is rather limited since the correspondence is only a logarithm. A small error in OD measurement will give a very large error in the readout of the phage concentration. However, the authors do not discuss the precision of the proposed method, which is a very important point if this method were to be used to quantify phage concentration. What is the expected error bar if one measures the lysis OD only once and reads the phage concentration out? Does it help to do many parallel OD curves and measure lysis OD with a smaller error bar? What percentage of difference in phage concentration can the method detect?"

In the original manuscript, our analysis of the accuracy and precision of OD-based phage measurements was unfortunately buried in the supplementary material. In addition to moving the information to the main text (lines 46-54 and **Figs. 2b-d**), we have now revised and expanded the analysis as detailed below.

First, regarding the logarithmic sensitivity of the method, it is true that the measurement is logarithmic in nature, in that the measured feature (lysis OD) reflects the log of the concentration. In our view, however, this is an advantage rather than a shortcoming: When using traditional plaque counting to quantify an unknown phage

sample, one has to plate serial dilutions of the sample to arrive at a countable number of plaques per plate[13–15]. This serial dilution is a bottleneck in the quantification of unknown samples, one that our approach overcomes by offering a dynamic range of multiple decades: ~9 for lambda in LBM, 5–9 for other phages and other growth media. Furthermore, as we describe below, the logarithmic sensitivity does not imply that the counting accuracy is limited to an order of magnitude. Rather, the typical accuracy is ~2 fold, and better than ~4 fold across different phage species and concentrations. If higher accuracy is needed, one can potentially combine the two phage-counting approaches, first using the OD-based method to infer the log concentration, then utilizing the required dilution for plaque counting. These points are now discussed in lines 206-212.

To improve the evaluation of accuracy and precision of our method, we now present the measurements of phage concentrations in samples of four different phages, (λ_{ts}, λ_{wt}, T5, and P1*vir*), each phage at three different concentrations, performed using both the OD-based protocol and standard plaque assay (**NEW Fig. 2b**, reproduced below). The experiment was a single-blind test, where one person prepared the samples and performed the plaque assay, and another person performed the OD-based measurements. Using a single linear calibration curve per phage, we found that the values obtained from the OD method are typically within two-fold of those obtained via plating, and at worse within four-fold (**NEW Fig. 2c**, reproduced below). As for the precision, we used the values obtained from two reading replicates of the plate-reader assay to calculate the coefficient of variation (CV). The typical CV is ~2, with higher CV values observed at lower phage concentrations (**NEW Fig. 2d**, reproduced below). Both the accuracy and precision can be moderately improved by interpolating between adjacent calibration points rather than using a single line (**NEW Supplementary Fig. 4**, reproduced below). Therefore, using several culture replicates, the OD-based method can reliably distinguish unknown samples having an approximately two-fold difference in phage concentration. The analysis above is now discussed in lines 46-54 and **Supplementary Methods, Section 4.5**.

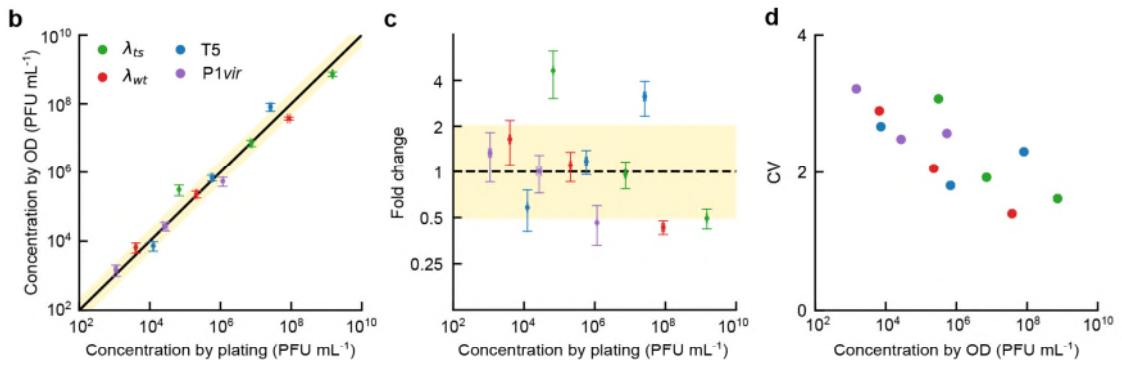

Fig. 2: The optical density (OD) at which massive lysis begins is used to measure the initial phage concentration.

[…] (**b**) Comparison of phage concentrations measured using the OD-based method and traditional plaque assay. Samples of λ_{ts}, λ_{wt}, T5, and P1*vir* (green, red, blue, and purple, respectively), each phage at three different concentrations, were enumerated using the two methods. Markers, mean; error bars, SEM from $n = 2$ culture replicates. Black line, $y = x$. Yellow shading, fold change ≤ 2 from the black line.

(**c**) The accuracy of OD-based phage counting. The fold change between the phage concentrations measured using the OD-based method and the plaque assay, calculated using the data in Panel **b**, is plotted. Markers, mean; error bars, SEM from $n = 2$ culture replicates. Yellow shading, fold change ≤ 2.

(**d**) The precision of OD-based phage counting. The coefficient of variation (CV) between the culture replicates ($n = 2$) for each sample is plotted.

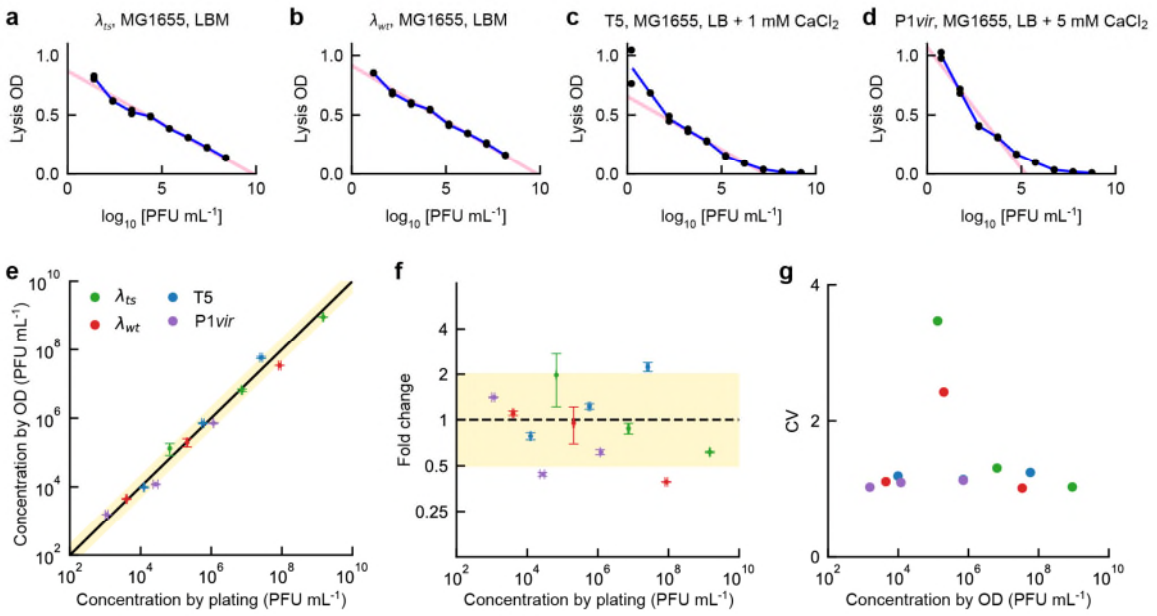

Supplementary Fig. 4: Accuracy and precision of OD-based counting when interpolating between adjacent calibration points.

(**a-d**) Calibration curves for (**a**) λ_{ts}, (**b**) λ_{wt}, (**c**) T5, and (**d**) P1*vir*. Markers, data. Pink lines, linear calibration curves (used in calculating the data shown in **Figs. 2c-e**). Blue lines, interpolation between adjacent calibration points (used in calculating the data shown in panels e-g below).
(**e**) Comparison of phage concentrations measured using the OD-based method and traditional plaque assay. Samples of λ_{ts}, λ_{wt}, T5, and P1*vir* (green, red, blue, and purple, respectively), each phage at three different concentrations, were enumerated using the two methods. Markers, mean; error bars, SEM from $n = 2$ culture replicates. Black line, $y = x$. Yellow shading, fold change ≤ 2 from the black line.
(**f**) The accuracy of OD-based phage counting. The fold change between the phage concentrations measured using the OD-based method and the plaque assay, calculated using the data in panel b, is plotted. Markers, mean; error bars, SEM from $n = 2$ culture replicates. Yellow shading, fold change ≤ 2.
(**g**) The precision of OD-based phage counting. The coefficient of variation (CV) between the culture replicates ($n = 2$) for a given sample is plotted.

"**[2.2]** The model is based in the cell number concentration, and the authors seems to assume the conversion factor that OD 1 is 10^9 CFU/ml (Supll. Material 6.1) without experimentally checking it. However, it is well known that cell size changes upon growth, especially close to the entropy to the stationary phase, and also depending on the growth media (faster growth gives bigger cells hence, the same OD means less number of cells per mL). This can affect the fitting and, hence, the inferred parameters for some factors."

In the original manuscript, we chose to ignore the non-constancy of OD-to-number conversion in an effort to simplify the model. In response to the reviewer's comment, we now consider this effect. Specifically, for infection and induction in LB-based media, we now describe the molar absorptivity of the cell (ε), which changes with its size[16] and hence with the growth rate[17]. Recall that in our model, the growth rate is a function of the nutrient concentration N. We therefore chose to describe ε too as a function of N. Briefly, we parameterized ε as a function of OD using the data of Sezonov *et al.*[17] (**NEW Supplementary Fig. 5a**, reproduced below), and used the curve to convert the OD vs. time data from uninfected cell cultures to cell density vs. time (**NEW**

Supplementary Fig. 5b, reproduced below). The latter was in turn used to parameterize cell growth using our multi-phase growth model. By combining the nutrient profile at different cell densities (obtained from the model, **NEW Supplementary Fig. 5b**) and the ε values at the respective densities, we obtained a relation between ε and N (**NEW Supplementary Fig. 5c**, reproduced below). This relation was then used to convert the model-predicted cell densities to predicted OD, and to fit the experimentally measured OD. This procedure is described in lines 72-74, lines 84-88, and **Supplementary Methods, Section 6.2**. We note that in minimal media (M9Glu, M9Mal), cell growth took place at an approximately constant growth rate up to massive lysis, irrespective of the initial phage concentration (**Supplementary Figs. 3h-i**). In light of that, we maintained the earlier simplifying assumption of a constant OD-to-number conversion.

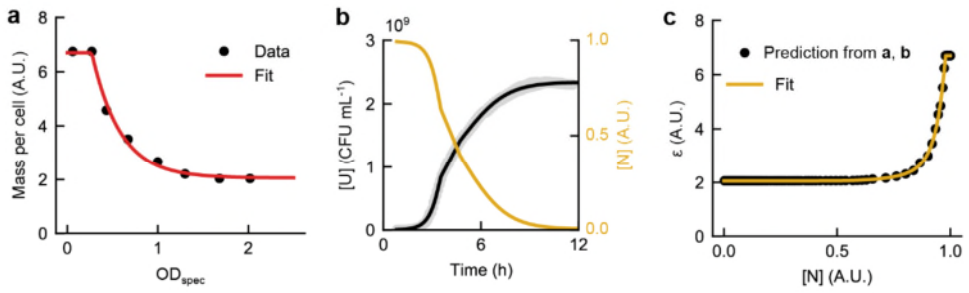

Supplementary Fig. 5: Parameterization of the cell density-to-OD conversion.

(**a**) Mass per cell as a function of OD_{spec}, adapted from Sezonov *et al.*[17], where mass per cell is defined as the ratio of OD_{spec} to the cell concentration, multiplied by 10^9.
(**b**) A model describing nutrient-dependent growth (black) captures the cell density dynamics of uninfected cultures (gray); gold, the inferred time-dependent nutrient abundance.
(**c**) A polynomial fit (gold) captures the relative absorptivity as a function of nutrient concentration (black). The data analysis procedure is described in **Supplementary Methods, Section 6.2**.

"**[2.3]** In figure 2, the authors tried to infer the latent period, burst size, and the rate constant for phage/cell encounter by fitting the model to OD and phage concentration curve.

[2.3-a] There is a fundamental question if the infected cells in the latent period contribute to the OD in the same way as uninfected cells. The last author previously showed impressive movies of cells infected by lambda going through the lysis process (Golding I. Single-cell studies of phage λ: hidden treasures under Occam's rug. Annual Review of Virology. 2016 Sep 29;3:453-72.), and those examples cells are clearly significantly longer than typical uninfected E. coli before the burst. The current model assumes that one infected cell represents the same OD as one infected cell, but this can be wrong if the cell size is significantly different, and that can affect the inference of the parameter."

As in the case of **comment 2.2** above, we originally ignored this feature for the sake of parsimony. Following the reviewer's comment, we tested whether the increased contribution to OD by infected cells would affect the model inference. To do so, we used the data in ref. [16], where the molar absorptivity (ε) of ampicillin-treated *E. coli* cells (~30 μm long) was reported to be 3-fold that of exponentially growing cells. We used this 3-fold factor in our model as the upper bound for the change in molar absorptivity of infected cells (see **Supplementary Methods, Section 6.9**). Considering the model version where r changes with growth rate, we found that incorporating this feature led to a modest ~2 fold change in the inferred values of r and B, and no change in τ, compared to the original model where infected and uninfected cells have the same molar absorptivity (**NEW Supplementary Fig.**

20c, reproduced below). Furthermore, the inferred value of the relative growth rate of the viral population, R, was almost unchanged (**NEW Supplementary Fig. 20d**, reproduced below), and the quality of fitting the OD dynamics, and of predicting phage dynamics, were not improved (**NEW Supplementary Figs. 20a-b**, reproduced below). Consequently, we decided not to incorporate any change in absorptivity of infected cells. This choice is now stated in lines 79-82 and **Supplementary Methods, Section 6.9**.

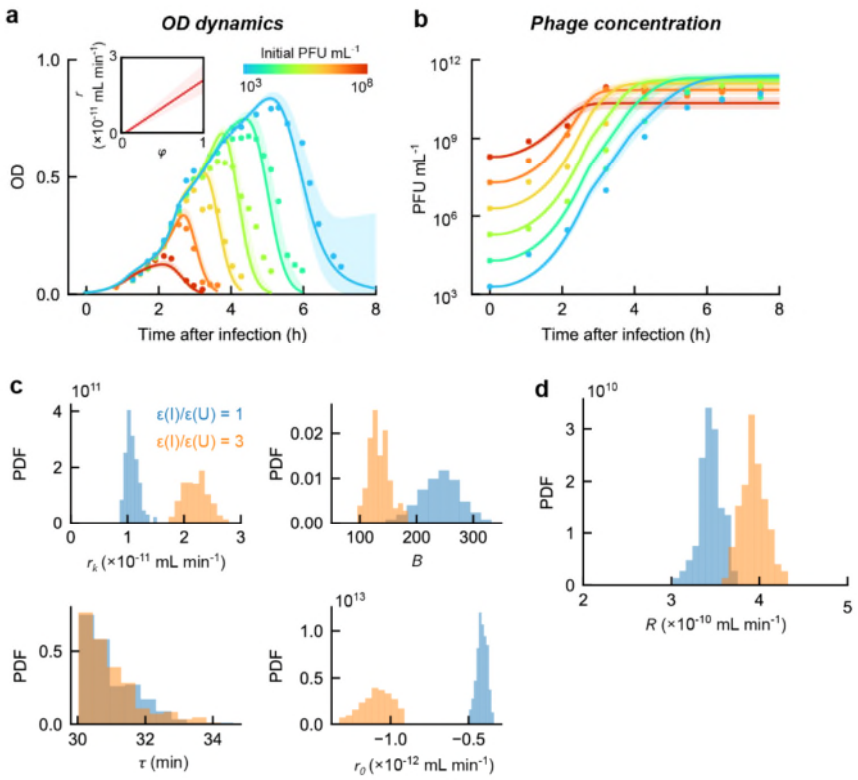

Supplementary Fig. 20: Modeling the increased length of infected cells.

(**a**) Model fitting for the OD dynamics using the "r-model", assuming the molar absorptivity (ε) of infected cells is three-fold of the uninfected cells. Colored markers, data from infection at different initial phage concentrations. Colored lines, best fit of the model. Colored shading, fits by the ensemble of parameters obtained using Markov chain Monte Carlo (MCMC). Inset, fitted r as a function of normalized instantaneous growth rate φ.
(**b**) Prediction of the phage dynamics. Colored markers, data from infection at different initial phage concentrations. Colored lines, model predictions from the best-fit parameters. Shared regions, model predictions from the ensemble of parameters. The fitting and prediction procedures are described in **Supplementary Methods, Section 6.9**.
(**c**) The distribution of parameter values, when the molar absorptivity of infected cells is the same as that of the uninfected cells (blue) or threefold of the uninfected cells (orange).
(**d**) The distribution of the relative growth rate of viral population (R) in the two models.

"**[2.3-b]** To infer the latent period, a model was fitted to the OD curve of phage-infected cultures from its deviation from the uninfected OD curve to the collapse using the model presented in 6.3 in the supplementary material. It is unclear how the initial condition for eq. (6.5) was set. If it was set so that all populations are in I1 at the lysis OD, then that is equivalent to assuming that all the cells were infected at the start of the fitting simultaneously (the peak of the OD curve). If so, even if my concern a) were not significant, the fit

underestimates the latent period; fit starts when the visible lysis starts to occur, so that means a significant number of cells were infected at lysis peak timing minus the latent period."

To address this concern, we now fit all three parameters (r, B, and τ) simultaneously, using the entire growth curve. This removes the implicit assumption of synchronized infection. As described in our response to **comment 2.0-a** above, we tested several model variants, in each of which one of the parameters is a linear function of the normalized instantaneous growth rate, and the slope and intercepts of that linear function are inferred. The new fitting procedure is described in lines 89-101 and **Supplementary Methods, Sections 6.3-6.5**. The revised fitting results are shown in **NEW Fig. 3c** and **Supplementary Fig. 7**, reproduced in **comment 2.0-a** above.

"A few more concerns regarding this fit are:

[2.3-b-i] The authors make a correlation curve between the instantaneous growth rate at the lysis OD and the inferred latent period, but as stated above, the actual infection should have happened over a period of time where the growth rate is continuously changing. Because the nutrient decreases over time in general, the latent period can still correlate with the growth rate at the lysis OD, but that does not mean that the instantaneous growth rate at that time determines the latent period. However, the authors assume this causality without deeper consideration."

Please see our response to **comment 2.0-b** above.

"**[2.3-b-ii]** The authors state that the fitted value of tau increases with the doubling time at the massive lysis and state it is T4 measurement in ref. 22. However, another measurement of T4 parameters in various steady-state growth reported different tendencies (Hadas H, Einav M, Fishov I, Zaritsky A. Bacteriophage T4 development depends on the physiology of its host Escherichia coli. Microbiology. 1997 Jan;143(1):179-85. : Parameter dependence is summarised in Rabinovitch A, Fishov I, Hadas H, Einav M, Zaritsky A. Bacteriophage T4 development in Escherichia coli is growth rate dependent. Journal of theoretical biology. 2002 May 7;216(1):1-4.). This should be discussed."

We thank the reviewer for bringing to our attention the Hadas study, which we found informative. Comparing it with ref. 22 (Nabergoj *et al.*) is illuminating: Despite using different methods to modulate the bacterial growth rate (chemostat growth in LB versus batch culture in different carbons sources), and different ways to characterize the infection parameters, when mapped to the same observable—the relative growth rate of the viral population, R—the two T4 studies identified a similar increasing trend for this parameter with growth rate (**NEW Supplementary Fig. 11**, reproduced in **comment 2.0-b** above), mirroring what we observe in the current work (**NEW Fig. 3f**, reproduced in **comment 2.0-a** above). As the reviewer pointed out in **comment 2.0-b** above, our current measurements were done under conditions where the growth rate changes over time, thus we cannot establish a causal link with the instantaneous growth rate. Nevertheless, we feel that the T4 data points in that direction, and make this argument in the revised text, lines 121-124 and 215-216.

"**[2.4]** The model presented in Fig.2 is used to fit the phage concentration curve in Fig. 2D.

[2.4-a] The model assumes that the phages are produced only after the cell lysis. However, the method states that to measure the phage concentration in Fig. 2D, the cells in the sample were lysed by adding chloroform. This allows the phages produced in the infected cells that have not yet burst also to be included in the phage count. Therefore, the data in Fig. 2D is not correspond to the free phage P in the model used in the fitting."

The reviewer is, of course, correct, and the chloroform procedure results in counting of phages from unlysed cells. In the model, we capture this feature by adding a contribution of B phages from each cell in the I_M population (i.e., in the last pre-lysis stage of infection; **Supplementary Methods, Section 6.6**). As explained in our response to **comment 2.0-a** above, we now use only the cell data for fitting, and the phage numbers are subsequently *predicted.* The fact that the model successfully captures the phage data (**Fig. 3e** and **NEW Supplementary Figs. 7e-f**, reproduced in **comment 2.0-a** above) suggests that our heuristic way of including the pre-lysis phage population is adequate.

"**[2.4-b]** I assume that the authors used the latent period for this fit based on the instantaneous growth rate and the correlation in Fig. 2C. This has the concern as stated in 2-ii); hence, the value used may be wrong."

As explained in our response to **comment 2.0-a**, the three parameters r, B, τ, are now fitted simultaneously. The inferred values are then used to predict phage dynamics, such as the data plotted in **Fig. 3e** and **NEW Supplementary Figs. 7d-f**.

"**[2.4-c]** The authors can still fit the curve despite the above uncertainties and state the best-fit parameters with very small error bars. This can be a sign of overfitting; because of a high degree of freedom and many parameters can compensate for each other, there may be a wide range of parameters that fit quite all right, but authors are only picking the best fit. In reality, the parameters are not as constrained as the error bars suggest. For example, the authors assume constant burst size, but a clear change in the burst size was observed when the growth rate was changed in the steady state growth condition in the Hadas paper mentioned above. For example, if the latent period prediction in Fig 2C is wrong but actually does not change much, but if burst size is reduced with growth rate, this may compensate. Overall, there are so many uncertainties in the model and the fit, and inferring parameters with the error bar that the authors present appears misleading."

We hope that our detailed response to **comment 2.0-a** above addresses these concerns.

"**[2.5]** In Fig 4, the authors inferred the growth rate dependence of the lysogenisation frequency and the spontaneous induction rate.

[2.5-a] For Fig. A-C, the authors plot a correlation between the frequency of lysogeny and the growth rate at the time when the phage is added. Again, as stated above, this is just a correlation."

As in the case of **comments 2.0-b** and **2.3-b-i** above, we agree that in our experiments, where the change in growth rate takes place over time, we cannot determine whether the change in behavior reflects a dependence on the instantaneous growth rate or on the culture's history, or both. We have revised the text to reflect this caveat (lines 225-227). Notwithstanding, and as we noted in the original manuscript, the idea that slow growth promotes lysogeny seems mechanistically plausible, considering that multiple regulatory interactions feed from the signaling molecules encoding information on cellular growth (ppGpp, cAMP), through cellular proteases (FtsH, Lon, RecA) and ribonucleases (RNase III), into the phage decision circuitry[18,19]. A dependence of lysogeny on growth rate is also plausible from the ecological angle, premised on the rationale that slower growing cells would have reduced capacity for a successful lytic reproduction. These matters are now discussed in lines 227-232.

"The model presented in Fig. S9 is inconsistent with their assumption of the lysogenisation frequency dependence upon growth rate and MOI.

[2.5-b] The model does not count the superinfection (though it is possible to construct such a model, where every infection to the infected state can move to another superinfected state), so the model does not know how many fraction of the infected cells experienced superinfections. Instead, the lysogenisation frequency is assigned based on the initially added phage concentration. This is another indication that the data is not constraining the model: A simple model actually reproduces the curves quite all right without the complex growth rate dependence or MOI dependence. That does not necessarily mean that the model and inferred parameters are close to the truth."

Our goal in presenting this oversimplified model was to show how it fails. As the reviewer notes, the model does not consider superinfection, and particularly the effect of MOI on the probability of lysogenization. While the model seemingly succeeds in capturing the observed cell dynamics, the fitting comes at the price of nonsensical inference: that the probability of lysogenization at each infection event depends on the initial conditions. This failure supports the argument, premised on the literature, that the dependence on MOI, as well as on growth rate, is critical for describing the emergence of lysogens. The reviewer's comment suggests that our use of the "straw model" created confusion rather than clarity, and we therefore decided to remove it.

"**[2.5-c]** For the induction rate, the authors assume there is no phage adsorption in this experiment. The method states that LB medium was "supplemented with 10mM MgSO4 and 0.2% glucose, the latter added to inhibit phage adsorption to cells (ref 13, 35)". In ref. 35, the effect on the adsorption rate to add glucose is at most factor 100 reduction, but it can be only factor 10. When the cell concentration is high and investigating time scale of hours, even a small adsorption rate can affect the phage number significantly. The authors should show that the adsorption is negligible in the concentration and time scale used in the condition used."

Following the reviewer's comment, we tested the effect of allowing adsorption of the released phages, at an efficiency 10-fold lower than in the maltose medium[20], on the "r-model", "B-model" and "τ-model". For each model, the parameters for r, B, and τ were inherited from the fitting of infection dynamics in LBM (**Supplementary Table 3**, reproduced in **comment 2.0-a** above). The spontaneous induction rate was assumed to be a linear function of the normalized instantaneous growth rate (φ), with the slope and intercept of that linear function as free parameters (see **Supplementary Methods, Section 8.2**).

As can be seen in **Fig. 5f**, **NEW Supplementary Fig. 17** and **Supplementary Table 5** (all reproduced below), in the absence of phage adsorption to glucose-grown cells, all three models reproduce the data, and the fitted induction rates all increase with the growth rate. When adsorption is introduced, the "B-model" cannot reproduce the data, while the "r-model" and "τ-model" are able to do so; for the "r-model" and "τ-model", the fitted induction rate increases with growth rate, exhibiting a similar trend to the models fitted without considering adsorption. Thus, the added feature does not affect the model's ability to capture the data, nor does it alter the conclusion that the spontaneous induction rate increases with the growth rate. This point is now made in line 182, lines 189-194, and **Supplementary Methods, Section 8.2**.

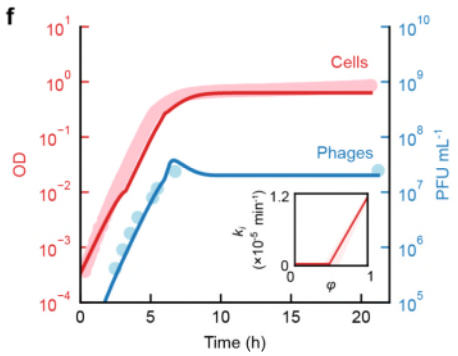

Fig. 5: The propensity to enter and maintain lysogeny increases as the bacterial growth slows down.

[…] (**f**) The OD (red) and the concentration of free phages (blue) during growth of lysogens. MG1655 λ_{ts} was grown at 30°C in LBM supplemented with 0.2% glucose. Markers, experimental data. Lines, fit of a model where the rate of phage-cell encounter (r) depends on the bacterial growth rate. Inset, the inferred rate of spontaneous induction (k_i) as a function of the normalized instantaneous bacterial growth rate (ϕ). For other model variants, see **Supplementary Fig. 17**.

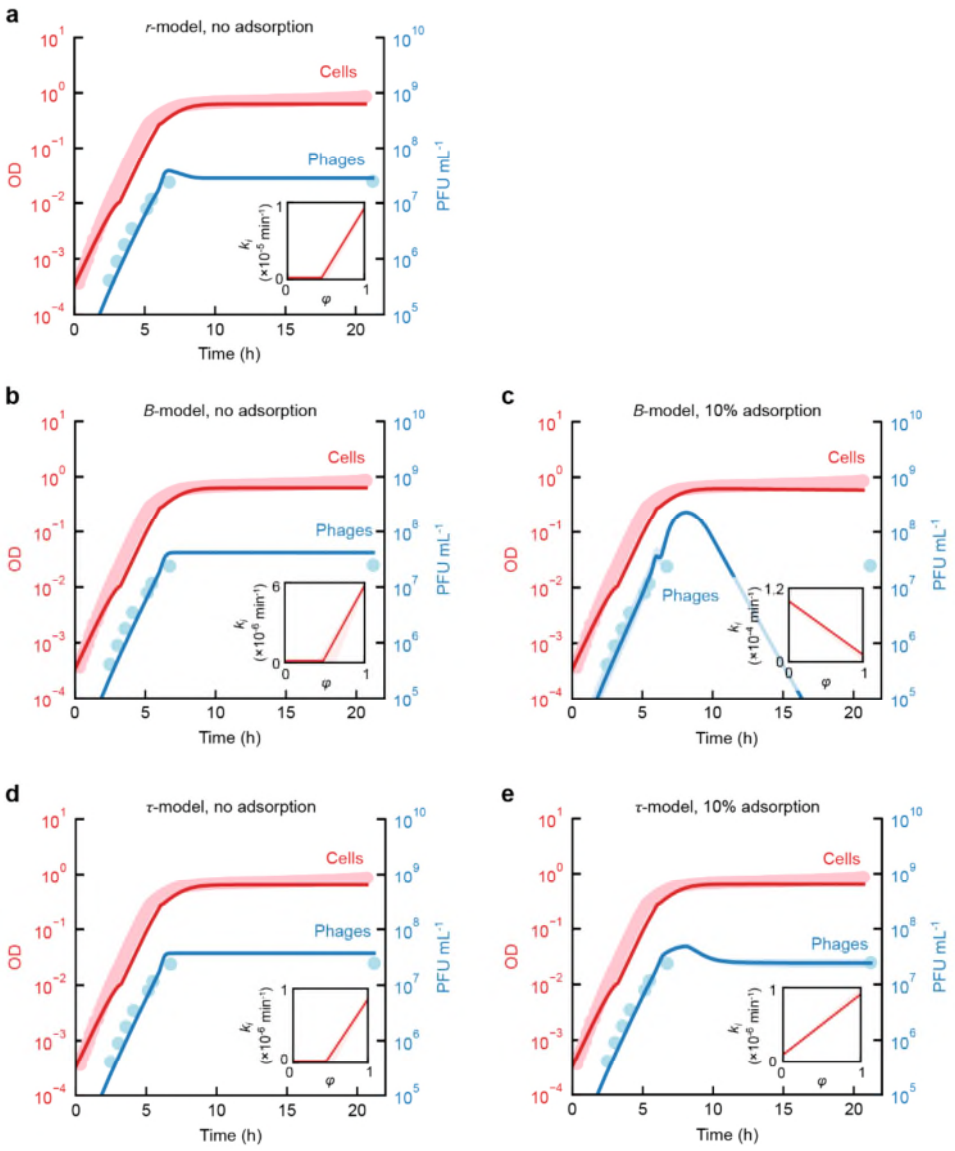

Supplementary Fig. 17: Modeling lysogen growth and phage dynamics using different assumptions.

Modeling OD (red) and phage concentration (blue) during growth of lysogens using different models. In each panel, markers, experimental data. Lines, model fitting. Shading, fits by the ensemble of parameters obtained using Markov chain Monte Carlo (MCMC). Inset, the inferred rate of spontaneous induction (k_i) as a function of the normalized instantaneous bacterial growth rate (φ). The fitting procedure is described in **Supplementary Methods, Section 8.2**. The fitted parameters are shown in **Supplementary Table 5**. For the "r-model" with a 10% adsorption rate as in LBM, see **Fig. 5f**. The model assumptions for each panel are as follows: (**a**) "r-model", without adsorption; (**b**) "B-model", without adsorption; (**c**) "τ-model", without adsorption; (**d**) "B-model", with a 10% adsorption rate as in LBM; (**e**) "τ-model", with a 10% adsorption rate as in LBM.

Supplementary Table 5: Fitted induction rates using different models

Model	Parameter	Range of prior	Best fit value	Range of ensemble of parameters
r-model + no adsorption	k_{i_k}	$[10^{-7}, 10^{-4}]$ min^{-1}	1.6×10^{-5} min^{-1}	$[1.5\times10^{-5}, 1.8\times10^{-5}]$ min^{-1}
	k_{i_b}	$[-10^{-4}, 10^{-4}]$ min^{-1}	-7.0×10^{-6} min^{-1}	$[-9.0\times10^{-6}, -6.2\times10^{-6}]$ min^{-1}
B-model + no adsorption	k_{i_k}	$[10^{-7}, 10^{-4}]$ min^{-1}	1.1×10^{-5} min^{-1}	$[1.0\times10^{-5}, 1.5\times10^{-5}]$ min^{-1}
	k_{i_b}	$[-10^{-4}, 10^{-4}]$ min^{-1}	-5.1×10^{-6} min^{-1}	$[-9.3\times10^{-6}, -4.1\times10^{-6}]$ min^{-1}
τ-model + no adsorption	k_{i_k}	$[10^{-7}, 10^{-4}]$ min^{-1}	1.5×10^{-6} min^{-1}	$[1.4\times10^{-6}, 1.8\times10^{-6}]$ min^{-1}
	k_{i_b}	$[-10^{-4}, 10^{-4}]$ min^{-1}	-6.4×10^{-7} min^{-1}	$[-9.4\times10^{-7}, -5.6\times10^{-7}]$ min^{-1}
r-model + 10% adsorption	k_{i_k}	$[10^{-7}, 10^{-4}]$ min^{-1}	2.1×10^{-5} min^{-1}	$[1.9\times10^{-5}, 2.7\times10^{-5}]$ min^{-1}
	k_{i_b}	$[-2\times10^{-5}, 2\times10^{-5}]$ min^{-1}	-1.0×10^{-5} min^{-1}	$[-1.5\times10^{-5}, -7.5\times10^{-6}]$ min^{-1}
B-model + 10% adsorption	k_{i_k}	$[10^{-7}, 10^{-4}]$ min^{-1}	-8.6×10^{-5} min^{-1}	$[-9.5\times10^{-5}, -8.6\times10^{-5}]$ min^{-1}
	k_{i_b}	$[-10^{-4}, 10^{-4}]$ min^{-1}	9.9×10^{-5} min^{-1}	$[9.4\times10^{-5}, 10.0\times10^{-5}]$ min^{-1}
τ-model + 10% adsorption	k_{i_k}	$[10^{-7}, 10^{-4}]$ min^{-1}	8.1×10^{-7} min^{-1}	$[7.7\times10^{-7}, 8.8\times10^{-7}]$ min^{-1}
	k_{i_b}	$[-10^{-4}, 10^{-4}]$ min^{-1}	1.0×10^{-7} min^{-1}	$[8.8\times10^{-8}, 1.2\times10^{-7}]$ min^{-1}

References for this Response Letter

1. Gutenkunst, R. N. *et al.* Universally Sloppy Parameter Sensitivities in Systems Biology Models. *PLoS Comput Biol* **3**, e189 (2007).
2. Foreman-Mackey, D., Hogg, D. W., Lang, D. & Goodman, J. emcee: The MCMC Hammer. (2012) doi:10.48550/ARXIV.1202.3665.
3. Bull, J. J. Optimality models of phage life history and parallels in disease evolution. *Journal of Theoretical Biology* **241**, 928–938 (2006).
4. Nabergoj, D., Modic, P. & Podgornik, A. Effect of bacterial growth rate on bacteriophage population growth rate. *MicrobiologyOpen* **7**, e00558 (2018).
5. Hadas, H., Einav, M., Fishov, I. & Zaritsky, A. Bacteriophage T4 Development Depends on the Physiology of its Host Escherichia Coli. *Microbiology* **143**, 179–185 (1997).
6. You, L., Suthers, P. F. & Yin, J. Effects of *Escherichia coli* Physiology on Growth of Phage T7 In Vivo and In Silico. *J Bacteriol* **184**, 1888–1894 (2002).
7. Basan, M. *et al.* A universal trade-off between growth and lag in fluctuating environments. *Nature* **584**, 470–474 (2020).
8. Gray, W. T. *et al.* Nucleoid Size Scaling and Intracellular Organization of Translation across Bacteria. *Cell* **177**, 1632-1648.e20 (2019).
9. Lazazzera, B. A. Quorum sensing and starvation: signals for entry into stationary phase. *Current Opinion in Microbiology* **3**, 177–182 (2000).
10. Xavier, K. B. & Bassler, B. L. Regulation of Uptake and Processing of the Quorum-Sensing Autoinducer AI-2 in *Escherichia coli*. *J Bacteriol* **187**, 238–248 (2005).
11. Sánchez-Clemente, R. *et al.* Study of pH Changes in Media during Bacterial Growth of Several Environmental Strains. in *Environment, Green Technology, and Engineering International Conference* 1297 (MDPI, 2018). doi:10.3390/proceedings2201297.
12. Ratzke, C. & Gore, J. Modifying and reacting to the environmental pH can drive bacterial interactions. *PLoS Biol* **16**, e2004248 (2018).
13. Adams, M. H. *Bacteriophages*. (Interscience Publishers, New York, 1959).
14. Sambrook, J. & Russell, D. W. *Molecular Cloning: A Laboratory Manual*. (Cold Spring Harbor Laboratory Press, Cold Spring Harbor, N.Y, 2001).
15. Clokie, M. R. J. & Kropinski, A. M. *Bacteriophages: Methods and Protocols*. (Humana Press, New York, 2009).
16. Stevenson, K., McVey, A. F., Clark, I. B. N., Swain, P. S. & Pilizota, T. General calibration of microbial growth in microplate readers. *Sci Rep* **6**, 38828 (2016).

17. Sezonov, G., Joseleau-Petit, D. & D'Ari, R. *Escherichia coli* Physiology in Luria-Bertani Broth. *J Bacteriol* **189**, 8746–8749 (2007).
18. Casjens, S. R. & Hendrix, R. W. Bacteriophage lambda: Early pioneer and still relevant. *Virology* **479–480**, 310–330 (2015).
19. Golding, I., Coleman, S., Nguyen, T. V. P. & Yao, T. Decision Making by Temperate Phages. in *Encyclopedia of Virology* 88–97 (Elsevier, 2021).
20. Schwartz, M. The adsorption of coliphage lambda to its host: Effect of variations in the surface density of receptor and in phage-receptor affinity. *Journal of Molecular Biology* **103**, 521–536 (1976).

Reviewer #2 (Remarks to the Author):

The authors have successfully followed up on my comments. In the revised manuscript, they have tested differently structured models and have clearly shown that the overall phage growth parameter, which could be attributed to different phage parameters, is what is constrained by data. The authors also resolved several uncertainties in the previous version of the manuscript by performing additional experiments. This revision has effectively resolved my concerns. I believe that the current version of the manuscript will contribute significantly to quantitative phage research.

Below is a minor comment.
The revised abstract states, “A mathematical model allows us to infer the phage-cell encounter rate, latent period, and burst size.” However, each parameter was not inferred as reliable since their growth rate dependence compensates for each other. Hence, this sentence may be misleading. Isn’t it better to state, e.g., “a mathematical model allows us to infer relative phage growth rate, which is a function of the phage-cell encounter rate, latent period, and burst size.”? I recommend that the authors reconsider the sentence.

Reviewer #2

"The authors have successfully followed up on my comments. In the revised manuscript, they have tested differently structured models and have clearly shown that the overall phage growth parameter, which could be attributed to different phage parameters, is what is constrained by data. The authors also resolved several uncertainties in the previous version of the manuscript by performing additional experiments. This revision has effectively resolved my concerns. I believe that the current version of the manuscript will contribute significantly to quantitative phage research.

Below is a minor comment.

The revised abstract states, "A mathematical model allows us to infer the phage-cell encounter rate, latent period, and burst size." However, each parameter was not inferred as reliable since their growth rate dependence compensates for each other. Hence, this sentence may be misleading. Isn't it better to state, e.g., "a mathematical model allows us to infer relative phage growth rate, which is a function of the phage-cell encounter rate, latent period, and burst size."? I recommend that the authors reconsider the sentence."

We have revised the sentence in question to read "Interpreting the measured dynamics using a mathematical model allows us to infer the phage growth rate, which is a function of the phage-cell encounter rate, latent period, and burst size".